3D Micron-resolution Laue Diffraction

Gene E. Ice
Oak Ridge National Laboratory, Oak Ridge TN 37831-6118

1.0 Introduction

A fundamental question of materials science is how atomic-scale interactions self-organize atoms into mesoscopic structures. This simple question is important because the physical behavior of most materials is dominated by mesoscale structure and dynamics. For example, self-organization is essential to understand grain-growth and deformation microstructure and to understand their effects on plasticity, strength, fracture, transport and other materials properties.

To understand how meso-structures arise, and how they influence materials behavior, it is essential to map *local* elemental composition, crystal/local structure, and geometrical/chemical defect distributions. In materials, this information is mathematically approximated by three-dimensional (3D) tensor fields, that are typically highly heterogeneous. For this reason, 3D quantitative probes are essential. X-ray microdiffraction is particularly interesting as it provides detailed *atomic-resolution* information about local crystalline structure correlated with the *mesoscale* (0.1-10 μm) real-space resolution of the probe. Furthermore unlike almost any other probe, x-ray microbeams can nondestructively characterize materials properties in three-dimensions and can observe mesoscale evolution as a response to underlying driving forces (e.g. stress).

1.1 The need for *polychromatic* microdiffraction

Although diffraction with micron-scaled beams can provide detailed structural information, *monochromatic* microdiffraction studies are complicated; to efficiently diffract microbeams from small volumes, samples must be simultaneously positioned with submicron precision and aligned with arcsecond angular accuracy. In polycrystalline materials, the penetration of x-rays into the sample further complicates data interpretation as more than one (or none) of the grains intercepted by the incident beam can diffract (Fig. 1a). If the sample is oriented to position one grain to satisfy a Bragg condition, the neighbor grains illuminated by the penetrating beam can be rotated into or out of the beam. This problem is exacerbated by the sphere-of-confusion errors in rotations of the sample (Fig. 1b). High-energy monochromatic beams that flood many grains can be used for mapping of crystal structures as described in the previous chapter (Poulsen Ch. 22: 3D X-ray Microscope) Here the spatial resolution is determined by the spatial resolution of the detector and by corrections for sphere-of-confusion in the sample rotations. Polychromatic beams however, have the advantage of requiring no sample rotations for diffraction studies. In this case spatial resolution is determined to a large degree by the beam size, which can be submicron and even nanoscale. Furthermore issues of strain or deformation on the measured diffraction volume have–at least in principle- a small effect.

With a polychromatic (Laue) approach however there is a completely different problem: an over abundance of diffraction with each subgrain volume diffracting into overlapping Laue patterns on the detector (Fig. 1c). The complexity of the overlapping Laue patterns is greatly reduced by the use of small x-ray beams that limits the number of subgrains illuminated and can be further simplified by an experimental approach called differential

aperture microscopy which resolves the single-crystal-like Laue diffraction from subgrain volumes along the illuminating beam. The theories behind differential aperture microscopy and polychromatic microdiffraction are described briefly below.

2.0 Theoretical basis for advanced polychromatic microdiffraction

2.1 Modified Ewald's Sphere Description of Laue Diffraction

Monochromatic diffraction is conceptually represented by an Ewald's sphere diagram (Chapter 15: Basics of Scattering Methods). *Laue diffraction* can be similarly modeled by a *modified* Ewald's sphere diagram as shown in Fig. 2. Bragg reflections for a crystal are indicated in reciprocal space by a reciprocal-space lattice that is aligned to the real-space orientation of the crystal (Chapter 15). A Bragg reflection is excited when the momentum transfer of an accessible diffraction direction for a particular wavelength matches a reciprocal space lattice co-ordinate. For a collimated monochromatic beam, possible momentum transfers in reciprocal space lie on the Ewald's sphere, and the sample must be precisely oriented to pass a reciprocal lattice point through the Ewald's sphere.

With Laue diffraction however, a finite bandpass creates a volume in reciprocal space between maximum and minimum Ewald's spheres (note that the centers of the limiting spheres lie along the incident beam direction but are displaced from each other). Bragg reflections that fall within this volume are excited and the directions of the Laue pattern peaks indictes the Bragg plane normals of the crystal. More exactly, the intensity in each pixel in a Laue image is proportional to a line integral through reciprocal space weighted by the incident beam spectral distribution[1].

2.2 Qualitative information: Phase, texture, elastic strain, dislocation density

With the understanding that Laue images represent radial line integrals in reciprocal space, microLaue images can offer immediate qualitative information about the sample volume illuminated by the beam.

2.21 Phase

For example, as shown in Fig. 3a, the image from a small high-symmety unit cell looks qualitatively distinct from that of a large or low-symmetry unit cell (Fig. 3b). Hence phase distributions can often be determined by mapping the number of reflections emanating from subgrain volumes within the sample.

2.22 Texture

Similarly microLaue patterns are highly sensitive to orientation and for good quality crystals can measure orientations to 0.001 degrees [2]. Therefore measurements of local grain orientations (texture) are easily made with 1 to 3 orders of magnitude better angular resolution than with typical electron probe measurements. For example, in Fig. 3c, the relative angle between crystal layers in an engineered high-temperature superconductor structure are easily determined. Furthermore these orientation measurements can be made tens to hundreds of microns below the sample surface so that the local texture in thin films, multilayers and true 3D samples can be studied.

2.23 Dislocation tensor

In addition, dislocations are Krivoglaz defects of the 2nd kind that introduce long-range rotations in the Bragg planes [3]so that sharp Laue spots are smeared (Fig 3d). Single images can be used to model the dislocation density and distribution through the illuminated sample volume [4], or microLaue images can be resolved by differential

aperture microscopy to determine the local Laue pattern within a submicron volume and the 3D distribution of lattice rotations can be used to unambiguously extract the local dislocation tensor [5].

2.24 Elastic strain tensor

Finally, changes in the angles between reflections can be used to determine the local elastic stress. The angles between reflections can be used to determine distortions of the unit cell shape. These distortions are described by the local deviatoric strain tensor [6]. At least 4 indexed reflections are needed to determine the deviatoric strain tensor (distortion of the unit cell shape). If the energy of one reflection is determined, then not only the unit cell shape but also its volume can be determined and the full strain tensor can be found by comparison to the undeformed unit cell.

3.0 Technical developments for an automated 3D probe

Although Laue diffraction is the oldest x-ray diffraction method [7], the recent extension to 3D imaging of crystalline structure has relied on the most modern developments in x-ray sources, optics and detectors [8]. To go beyond a conceptual tool to an automated 3D probe for mapping crystal structure, five elements have been assembled in the “first-of-its-class” 3D X-ray Crystal Microscope deployed on station 34-ID-E at the Advanced Photon Source (Fig. 4) . These are (a) an ultra-brilliant x-ray source, (b) a nondispersive monochromator that can be cycled between monochromatic and polychromataic status, (c) nondispersive focusing optics with submicron resolution, (d) a scanning-wire differential aperture (Fig. 5), and (e) a high-resolution area detector. The purpose and performance of each element is described briefly below.

3.1 Source

An ultra-brilliant synchrotron source is the first essential element for automated polychromatic microdiffraction. The combination of small beam size and good collimation needed for simultaneously good real-space and momentum transfer resolution greatly restricts the phase space of the useable beam. This makes it important that the source have high brilliance (photons/s/mm^2/mrad^2/eV) over the required bandpass, but also means that the source emittance (size^2 $*$ divergence^2) can be small. A type A undulator at the APS has about 12 (4) orders of magnitude greater x-ray brilliance for monochromatic experiments and about 10 (2) orders of magnitude greater brilliance for wide-bandpass measurements than a laboratory (bend magnet synchrotron) source (Fig. 6). This high brilliance allows for microLaue images to be collected in milliseconds from many samples. Even though the undulator source is intrinsically highly collimated with a relatively small source, on 34-ID-E only about 0.1% of the total beam emittance is used in the polychromatic microbeam. This makes it possible to field many polychromatic beamlines on one undulator source.

Bend magnet sources can also be successfully used for polychromatic microdiffraction despite their lower overall brilliance. Currently the performance of polychromatic microdiffraction is influenced more by the speed of the detector readout than by the counting statistics in the Laue images. Sources that are only a factor of 100 lower in integrated brilliance can therefore do much of the science that is done with an undulator source and can be optimized for particular experiments to achieve very high performance.

3.2 Microbeam monochromator

A microbeam monochromator is the second important element of a polychromatic microdiffraction system. The monochromator allows for measurements of the full strain tensor. As described above, Laue images record radial line integrals through reciprocal space. Strain is determined by comparing the measured unit cell shape to the shape of an undistorted unit cell. Laue images cannot however distinguish between unit cells with slightly different volumes but the same shape. Therefore in order to determine the full strain tensor, it is important to measure the energy of one reflection. Of course the deviatoric strain tensor, which is most sensitive to shear stains can be measured without an energy measurement. On station 34-ID-E the microbeam monochromator can be translated into or out of the beam so the beam incident on the focusing optics is either polychromatic or monochromatic. The design also maintains a fixed offset independent of x-ray energy or bandpass [9].

The 34-ID-E monochromator utilizes a two-crystal fixed exit design with a small (~1 mm) offset. The polychromatic beam is taken from ~1 mm above the beam axis and the monochromatic beam is taken from near the beam axis (Fig. 7a). This optimizes the effective beam brilliance of the undulator source when used for monochromatic measurements and delivers a more uniform energy distribution for polychromatic experiments. Beamline 7 at the ALS uses a 4 crystal design that is intrinsically zero offset (Fig.7b). Beamlines planned for the Canadian Light Source and the Australian light source will use another trick that utilizes mirrors in addition to the crystals to switch between co-axial polychromatic or monochromatic beams (Fig. 7c). This design combines the simplicity, high-throughput and ease of use of a two-crystal monochromator with the advantages of an intrinsically zero offset dispersion-free design.

3.3 Nondispersive focusing optics

Nondispersive focusing optics *are the* essential element for polychromatic microdiffraction. On 34-ID-E, total external reflection Kirkpatrick Baez mirrors are used to focus to an ~300 x 500 nm^2 focal spot. The mirrors are fabricated by profile coating on ultra-smooth substrates [10,11]. Kirkpatrick-Baez optics are rapidly developing with hard x-ray nanoprobe optics suitable for polychromatic *nano*odiffraction having been demonstrated [11,12].

3.4 Area detector

An area detector to record the Laue pattern is also an essential element of a polychromatic microdiffraction station. Unlike fluorescence microscopy it is important that the scattering is out of the ring plane to improve the reflectivity of the polarized incident beam. On 34-ID-E and other (2D) polychromatic microdiffraction beamlines the detector is typically aligned at 90º to the incident beam. This geometry is a compromise that allows for simple sample alignment with reasonable reflectivity of x-rays between 10 and 20 keV (Fig. 4). The nominal 90º scattering angle also optimizes the penetration depth of elastically scattered x-rays for a given absorption coefficient.

A detector optimized for polychromatic microdiffraction is quite distinct from area detectors used in protein crystallography and other more common x-ray applications. For example, extremely linear pixel spacing is important to measure strains to 0.01%. Similarly large dynamic range, low readout noise, fast readout and low point-spread functions are all important. Readout speed is particularly important to collect meaningful 3D images in a reasonable time.

3.5 Differential aperture

The final element for a *3D* X-ray Crystal Microscope is a differential aperture. The differential aperture deconvolves the Laue patterns from subgrain volumes along the incident beam [5]. The principle of differential aperture microscopy is indicated in Fig. 5. A smooth high Z wire is passed near the surface of the sample (within ~200 μm). The wire is calibrated prior to the measurement so that its position is precisely known relative to the incident beam and the axis of the detector. As the wire moves along the sample surface, it occludes rays that are collected at the detector. The intensity as a function of wire position is observed for each pixel. The derivative of the measured intensity/wire step in each pixel is sum of a positive and negative images of the intensity distribution along the wire that reaches that particular pixel separated by the diameter of the wire. By ray tracing back from the pixel and wire locations, and taking into account small effects due to the angle of the intercepted beam, the origin of the intensity into each pixel can be mapped with submicron precision along the incident beam. A picture of the 3D X-ray crystal microscope on 34-ID-E is shown in Fig. 8 and a close up of the differential aperture is shown in Fig. 5. Efforts are now underway to accelerate differential aperture microscopy with multiple wires and more intelligent step scans.

3.6 Software

Although Laue diffraction is a long-established technique, until recently, no software existed to allow for automated mapping of multiple grains, for differential aperture microscopy or for precision determination of strain and modeling of deformation parameters. This software is still a work in progress, but is now the subject of an international effort to develop a standard package that will foster polychromatic microprobes on beamlines around the world. Existing software packages are described in

various references [6,13] and more advanced user-friendly software is under development.

4.0 Research Examples

The mission of station 34-ID-E is centered on fundamental investigations of long-standing issues in materials science. These issues include grain growth and 3D organization in polycrystalline materials; 3D dynamics of mesoscale structures; and fundamental assumptions in materials physics modeling. Studies of 3D organization underway include measurements of colony structure in processed materials and studies of fractal misorientation in deformed materials including the development of dislocation hierarchical structures. Other studies of 3D structures include measurements of percolation and diffusion behavior.

Studies of dynamics underway include 3D local growth of grains, measurements of ripening and measurements of anomalous grain growth (i.e. Sn whiskers). Other measurements include studies of nucleation sites, the role of deformation energy and elastic stress in grain nucleation, and grain/ subgrain rotations during deformation as a function of global and local environmental conditions.

Fundamental assumptions are being tested by experiments that include; mapping of intra- and inter-granular stresses to guide our understanding of the constitutive equations of materials near grain boundaries and other interfaces; measurements of grain boundary shear versus habit; and measurement of deformation scaling laws in three-dimensions.

4.1 3D Grain boundary networks

How grain boundary/polycrystalline networks interact to applied forces and environmental conditions is a central materials challenge of the 21st century. Modelers want to know the constitutive equations at grain boundaries, and how they change with boundary type. This information impacts efforts to model materials behavior and to engineer ideal microstructures for applications ranging from corrosion resistance to high strength. Similarly, synthesis and processing control of grain boundary distributions is an area of active research with particularly complex issues for nanoscale and advanced layered structures.

Polychromatic microdiffraction allows for unprecedented testing of longstanding assumptions regarding grain boundaries. For example, in coincident site lattice (CSL) theory, grain boundaries are considered to have lower energy if some of the lattice sites the neighbor grains overlap [14]. The lattice is assigned a number, Σ, which is the inverse of the fraction of shared sites; if 1/3 of the sites are shared then Σ equals 3. According to theory, high Σ boundaries can only have a slight misorientation because the energy minimum for high Σ boundaries is small and the subsequent energy well minimum is shallow. The good angular precision of polychromatic microdiffraction allows for detailed tests of this and other predictions of CSL theory. Preliminary measurements actually indicate an opposite trend in he distribution of lattice misorientations near CSL boundary conditions; measured misorientations from coincident site lattice boundaries increases with Σ. Other interesting questions which can be addressed include the role of curvature and faceting in grain boundaries. Grain boundary normals should have lower

energy in ideal CSL directions. However curved surfaces can also lower energy. Here the role of faceting may allow for energy minimization and studies are underway to study how 3D surfaces accommodate competing processes toward energy minimization. For example Fig. 9 shows a step in the surface of a polycrystalline Ni sample at a grain boundary triple junction as well as grain boundary grooving. Polychromatic microdiffraction is certain to shed new light on grain boundaries and on how grain boundaries effect materials behavior.

4.2 Deformation behavior and grain boundaries

Most theories of deformation are based on the crystallographic orientation of grains with respect to the applied load; the orientation controls the critical-resolved shear stress along slip systems. These theories have now been tested for the first time with the use of high-energy x-ray microdiffraction as described in Ch. 22. However, local environments also effect deformation behavior. For example, Pang [15] has recently studied rotations *across* grain boundaries before and after deformation. Her findings show a strong correlation between grain boundary angle and misorientation magnitude, and finds that coincident site lattice boundaries have a much different relationship to deformation than other boundary types (Fig. 10). Indeed deformation behavior near surfaces and interfaces appears to be quite distinct from the behavior near the center of grains [16].

4.3 Deformation in single crystals

Although the deformation of materials appears to have important complexity introduced by the presence of grain boundaries, there is strong evidence that even in single crystals

our understanding of deformation is a work in progress. For example, dislocations tend to organize into mesoscale dislocation walls and cells with scaling laws that extends over many orders of magnitude of deformation. Measurements of single-crystal surface roughening have identified self affine (fractal) behavior in point-to-point surface roughening of single crystals that extends over decades in length [17]. With polychromatic microdiffraction we can now measure misorientation and the development of 3D deformation structure to test theoretical predictions of deformation theories and to understand how bulk deformation compares to the surface behavior. Pang [18] has tested misorientation *both* at the surface and in the bulk to determine whether the surface observations are indicative of the bulk behavior or are somehow restricted to the near surface region. Her measurements find that the Hurst coefficient is sensitive to both depth and crystallographic orientation/strain load(Fig. 11). These studies are certain to provide new information about deformation in single crystals that can be directly compared to finite element and molecular dynamics models.

4.4 Grain Growth on Surfaces and In Three Dimensions

The penetrating nature of x-ray microdiffraction allows for precision measurements of thin-film growth, that correlate to the underlying substrate. For example, Budai [19] has explained the transition between “good” and “bad” growth of high temperature superconducting films on textured Ni substrates by demonstrating how the growth mechanism changes with temperature. Similarly Barabash [20-21] has studied defects in GaN thin films grown on patterned Si and SiC substrates (Fig. 12). Her results clarify how defects are introduced as a response to thermal and lattice mismatch strains.

More generally, the nondestructive nature of polychromatic microdiffraction enables a fundamentally new approach to the study of grain growth in three dimensions. Previous studies of grain growth have been limited to 2D growth, have depended on statistical information to understand how grains compete for material during grain growth, or have studied individual grains with little information about the local environment. Budai [22] has recently demonstrated that 3D images of grain structure can be measured and that grain growth can be observed before and after thermal annealing steps. The high angular precision of the measurements allows for a detailed study of how grain and subgrain boundaries are annealed out. Because the local environment-including the local stress state- can be measured, theories of grain growth can be directly compared to observed local movement of boundaries (Fig. 13)

4.5 Anomalous Grain Growth

In addition to normal grain growth, there are very interesting and technologically important cases where anomalous grain growth occurs. For example, Sn films are important as a low toxicity alternative to Pb. However, Sn films can spontaneously grow whiskers that can short circuit electronics. The mechanism behind this phenomena has been the subject of intense speculation and study. Polychromatic microdiffraction allows for detailed measurements of the environment and crystallographic nature of individual Sn whiskers. For example as shown in Fig. 14, an orientation map through a Sn film shows individual Sn grains and shows the presence of whiskers extending out from the surface. These whiskers are observed to include a range of crystallographic orientations and to include cases where the whisker is polycrystalline. Furthermore, the elastic strain

state in and near the grain can be measured to test theories of grain growth. Results from these experiments are certain to provide essential new information about anomalous grain growth in Sn films and shows the potential for addressing anomalous grain growth in a range of materials.

5.0 Future Prospects and Opportunities

Because polychromatic microdiffraction is still an emerging new field, research opportunities currently swamp available facilities. Extensive studies of the electromigration response of electronic interconnects has revealed the importance of deformation in the electromigration process [23]. Similarly measurements of domain wall structures, stresses in implanted materials, fracture, minor phases and precipitates, phase transitions and interface phases will all contribute to our understanding of materials behavior. Recent measurements to identify tiny microcrystalline grains inside bulk amorphous substrates, demonstrates an ability to test how materials segregate and accommodate metastable equilibrium under rapid annealing [24].

As equipment and techniques improve, the range of possible experiments will also increase. Faster detectors, detectors with energy resolution and smaller beams will all extend experimental possibilities. We envision in the near future, for example, a gain of at least a factor of 100 in data acquisition speed and an improvement of a factor of 10 in spot size (500 nm to 50 nm). With these capabilities, studies of nanocrystalline materials and studies of grain boundary morphology and faceting will become routine. In addition,

improved control of beam properties will allow for detailed studies of defects in micron-scaled volumes [25]. This will greatly accelerate diffuse measurements of defect properties and will allow point defect concentrations to be associated with mesoscale defects distributions.

Acknowlegement

This chapter would not have been possible without the efforts of many collaborators. These include, J.-S. Chung, W. Lowe, B.C. Larson, J.D. Budai, J.Z. Tischler, W. Liu, W. Yang, J.W.L. Pang, F. J. Walker, A. Khounsary, L. Assoufid, A. Macrander and R.I. Barabash. Work sponsored by the U.S. Department of Energy, Division (DOE), Division of Materials Sciences and Engineering. Oak Ridge National Laboratory (ORNL) is operated by UT-Battelle, LLC, for the U.S. Department of Energy under contract DE-AC05-00OR22725. Experiments were performed on Unicat beamline 34-ID at the Advanced Photon Source Argonne Il. Both 34-ID and the APS are supported by the DOE Office of Basic Energy Science.

The submitted manuscript has been authored by a contractor of the U.S. Government under contract No. DE-AC05-00OR22725. Accordingly, the U.S. Government retains a nonexclusive, royalty-free license to publish or reproduce the published or reproduce the published form of this contribution, or allow others to do so, for U.S. Government purposes.

References

1. R. Barabash, G. E. Ice, B. C. Larson, G. M. Pharr, K.-S. Chung, and W. Yang, "White Microbeam Diffraction from Distorted Crystals," *Appl. Phys. Lett*. **2001** *79*, 749-751.
2. W.G. Yang, B.C. Larson, G.E. Ice, J.Z. Tischler, J.D. Budai, K.S. Chung, W. Lowe ,"Spatially resolved Poisson strain and anticlastic curvature measurements in Si under large deflection bending", *Appl. Phys. Lett.* **2003** *82*, 3856-3858.
3. R.I. Barabash, G.E. Ice and J.W.L. Pang, "Gradients of geometrically necessary dislocations from white beam microdiffraction", *Mat. Sci. and Eng. A* **2005** *400*, 125-131.
4. R. I. Barabash, G.E. Ice, and F.J. Walker, "Quantitative microdiffraction from deformed crystals with unpaired dislocations and dislocation walls", *J. Appl. Phys*. **2003** *93*, 1457-1464.
5. B. C. Larson, W. Yang, G. E. Ice, J. D. Budai, and J. Z. Tischler, "Three-Dimensional X-Ray Structural Microscopy with Submicrometre Resolution," *Nature* **2002** *415*, 887-891.
6. J. S. Chung and G. E. Ice, "Automated Indexing for Texture and Strain Measurements with Broad-Bandpass X-ray Microbeams," *J. Appl. Phys*. **1999** 86, 5249-5256.
7. M. von Laue, "Nobel Lecure", **1915** http://nobelprize.org/physics/laureates/1914/laue-lecture.pdf.
8. W. Liu, G.E. Ice, B.C. Larson, W. Yang and J. Tischler, "The 3D X-ray Crystal Microscope: A new tool for Materials Characterization", **2004** *Met and Mat. Trans. A. 35A*, 1963-1967.

9. G. E. Ice, J.-S. Chung, W. Lowe, E. Williams, and J. Edelman, “Small-displacement Monochromator for Microdiffraction Experiments,” *Rev. Sci. Inst.* **2000** *71*, 2001-2006.

10. C. Liu, L. Assoufid, R. Conley, A.T. Macrander, G.E. Ice and J. Z. Tischler, ”Profile Coating and its application of Kirkpartrick-Baez Mirrors”, *Opt. Eng*. **2003** *42*, 3622-3628.

11. W. Liu, G.E. Ice, J.Z. Tischler, A. Khounsary, C. Liu, L. Assoufid, A.T. Macrander, :Short focal length Kirkpatrick-Baez mirros for a hard x-ray nanoprobe”, Rev. Sci. Inst. **2005** 76 113701(1-6).

12. K. Yamauchi, K. Yamamura, H. Mimura, Y. Sano, A. Saito, A. Souvorov, M. Yabashi, K. Tamasaku, T. Ishikawa and Y. Mori, “Nearly diffraction-limited line focusing of a hard-X-ray beam with an elliptically figured mirror”, J. Synch. Rad. **2002** *9*, 313-316.

13. N. Tamura, A.A. Macdowell, R. Spolenak, B.C. Valek, J.C. Bravman, W.L. Brown, R.S. Celestre, H.A. Padmore, B.W. Batterman and J.R. Patel, J. of Synch. Rad. **2003** *10*, 137-143.

14. W. Bollman, Crystal Lattices, Interfaces, Matrices: An extension of crystallography”, **1982** published by the author.

15. Pang, J. W. L., Ice, G.E. and Liu, W., "Inhomogeneous deformation behavior in intercrystalline regions in polycrystalline Ni", April **2006** accepted by Acta Mater

16. Pang, J. W. L., Barabash, R., Liu, W., and Ice, G.E., “Determination of Deformation Inhomogeneity in Polycrystalline Ni under Uniaxial Tension with 3D X-ray Microscope,” TMS Letters, **2004** 1 5-6.

17. M. Zaiser, F.M. Grasset, V. Koutsos, E.C. Aifantis, “Self-affine surface morphology of plastically deformed metals “ Phys. Rev. Lett. **2004** *93* 195507(1-4).

18. Pang J.W. L., Ice, G.E. and Liu, W., “ Single-crystal fractal misorientation as a function of depth and crystallography after deformation” **2006** in preparation.

19. Budai JD, Yang WG, Tamura N, Chung JS, Tischler JZ, Larson BC, **Ice GE**, Park C, Norton DP, **“**X-ray microdiffraction study of growth modes and crystallographic tilts in oxide films on metal substrates”, *Nature Materials* **2003** *2*, 487-492.

20. R.I. Barabash, O.M. Barabash, G.E. Ice, C. Roder, S. Figge, S. Einfeldt, D. Hommel, T.M. Katona, J.S. Speck, S.P. DenBaars and R.F. Davis, “Characterization of crystallographic properties and defects via X-ray microdiffraction in GaN (0001) layers”, *Physica Status Solidi* (a), **2006** *203*, 142-148.

21. R.I. Barabash, G.E. Ice, W. Liu, S. Einfeldt, A.M. Roskovski, R.F. Davis, “Local strain, defects and crystallographic tilt in GaN(0001) layers grown by maskless pendeo-epitaxy from X-ray microdiffraction”, *J. Appl. Physics,* **2005** *97*, 013504(1-5).

22. J.D. Budai, “Three-dimensional micron-resolution x-ray Laue diffraction measurement of thermal grain-evolution in aluminum”, Mat. Sci. Forum **2004** *467,* 1373-1378.

23. R.I. Barabash**,** G.E. Ice, N. Tamura, B.C. Valek, J. C. Bravman, R. Spolenak and J.R. Patel, “Quantitative analysis of dislocation arrangement induced by

electromigration in a passivated Al (0.5wt% Cu) interconnects", *J. Appl. Physics*, **2003** *93*, 5701-5706.

24. E. Miura, G.E. Ice, E. D. Specht, J.W.L. Pang, H. Kato, K. Hisatsune, A.Inoue, "X-ray Study Of Pd40Cu30Ni10P20 Bulk Metallic Glass Brazing Filler For Ti-6Al-7Nb Alloy" proceedings THERMEC2006 (International conference on processing & manufacturing of advanced materials) 2006 July 4-8, Vancover BC, Canada
25. G.E. Ice, R. I. Barabash, and W. Liu, "Diffuse X-ray scattering from tiny sample volumes", **2005** *220*, 1076-1081.

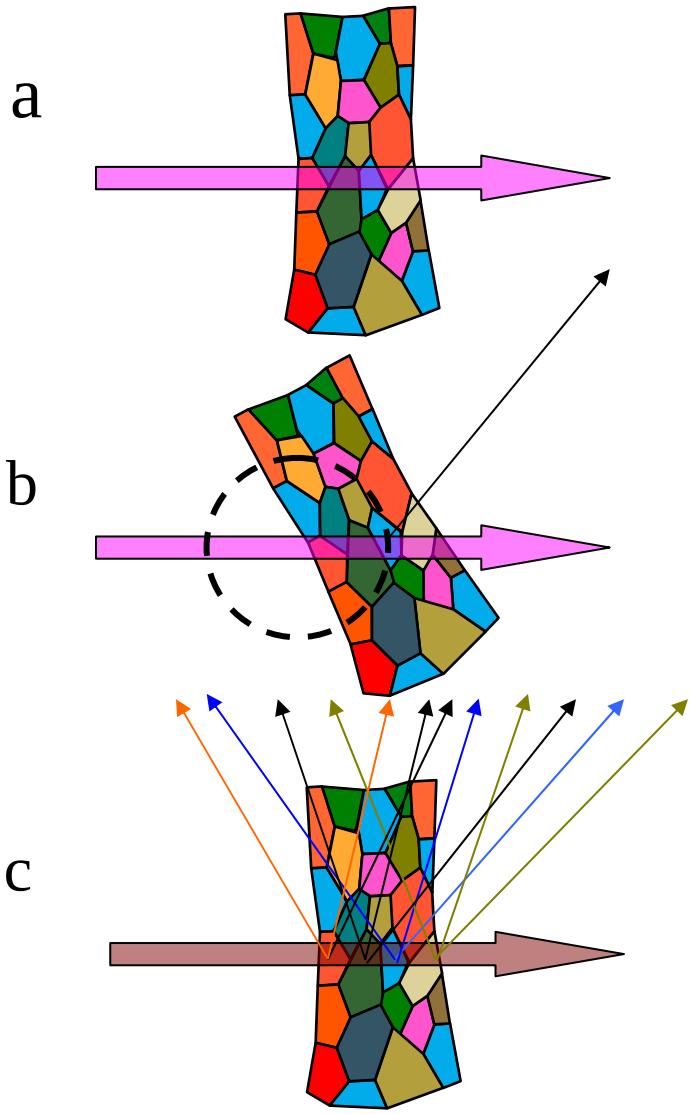
a
b
c

Fig. 1 a. A monochromatic x-ray beam has a low probability of diffracting from an arbitrary crystal grain orientation. b. If the sample is rotated to orient a grain for Laue diffraction the grain moves within the instrumental sphere-of-confusion even if it is centered on the goniometer rotation axis. Grains away from the rotation axis are in the incident beam path over an even smaller angular range. c. With a polychromatic beam, the subgrain volumes intercepted by the incident beam generate Laue patterns that overlap at the detector.

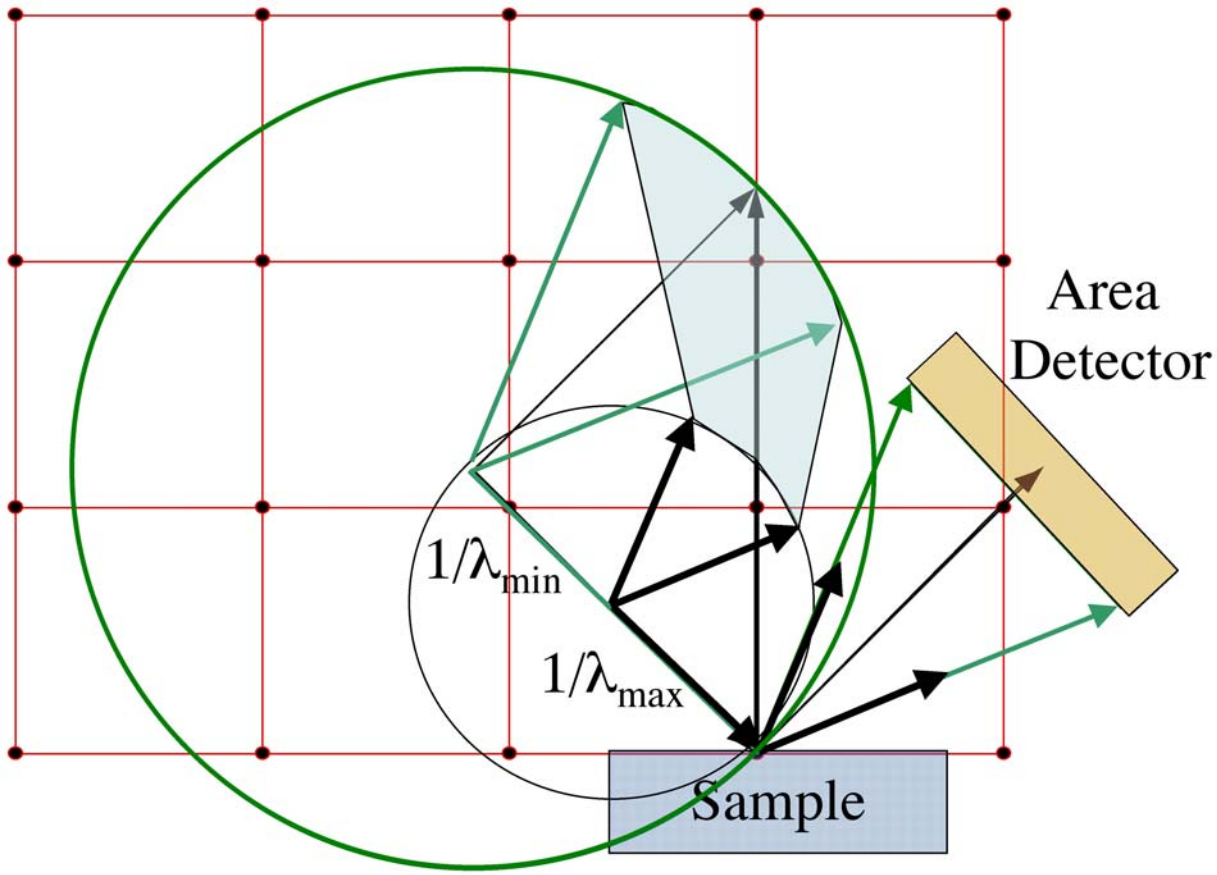

Fig. 2. A two dimensional modified Ewald's sphere diagram. In reciprocal space, the momentum of the an x-ray beam depends on its direction and wavelength. For short wavelength (green) the momentum is larger than for large wavelength (black). The momentum transfer is simply the vector difference between the final and incident x-ray momentums. For a fixed wavelength this lies on a sphere. The centers of the spheres for different wavelengths lie along the incident beam direction and are the spheres touch at the 0,0,0 position (no momentum transferred).The Laue pattern observed by an area detector is made up of radial line integrals through reciprocal space. Lattice points that lie within the bounds of the minimum and maximum Ewald's spheres contribute to the line integral.

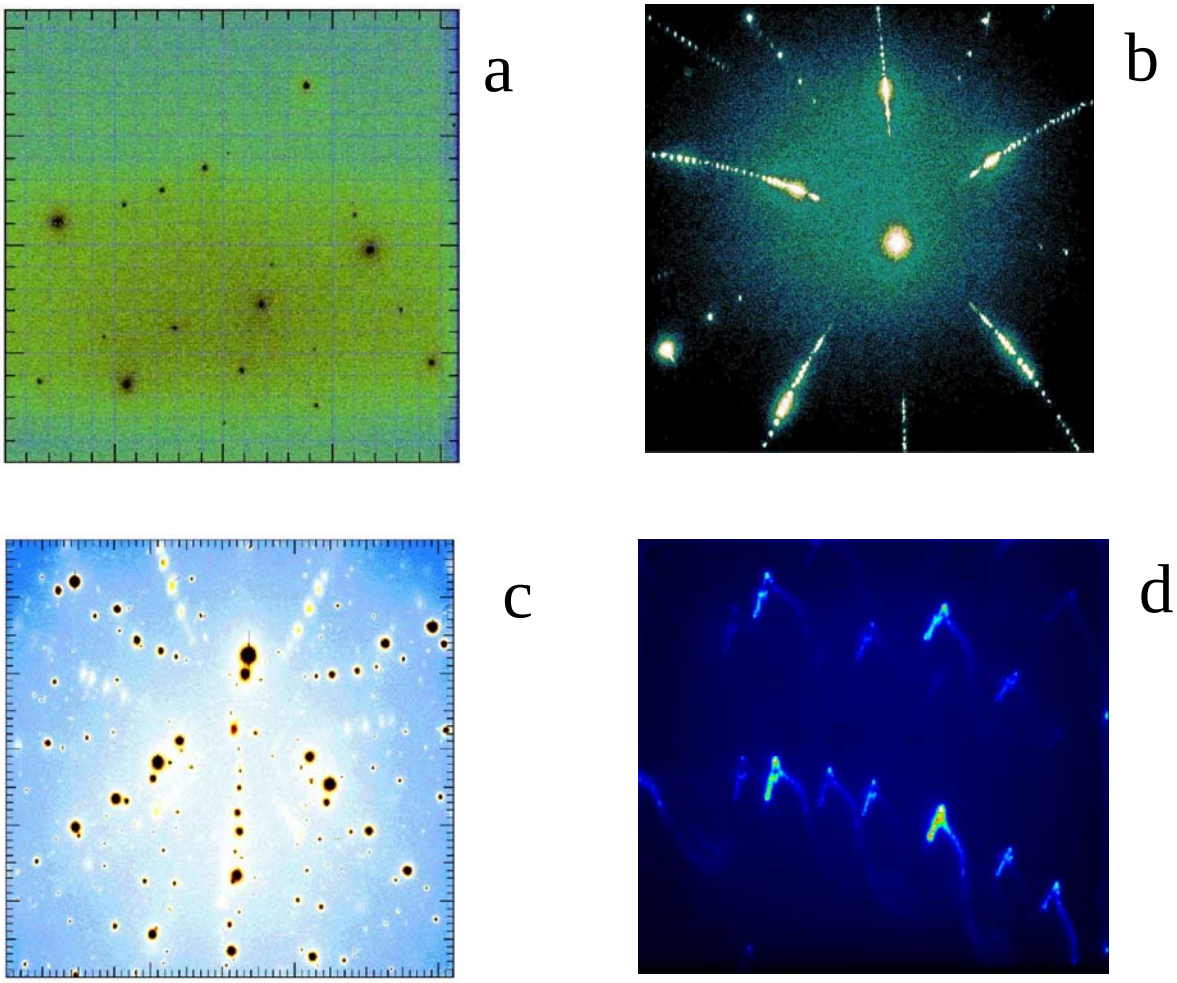

Fig. 3. (a) Laue pattern from a $Ni_{80}Fe_{20}$ single crystal. The small unit cell and high symmetry face-center-cubic (FCC) real-space lattice results in a sparse body-center-cubic (BCC) reciprocal-space lattice and consequently only a few Laue spots are detected. (b). Overlapping Laue patterns from a GaN film on a SiC single crystal. The two patterns are superimposed because the GaN film is crystallographically aligned to the SiC substrate. (c) High temperature superconducting film with buffer layer on a Ni single crystal. There are actually three patterns in the Laue image: one from the substrate and two from the two films. The patterns are at slightly different orientations due to crystallographic tilt between the layers. (d) Deformed Ni crystal shows a dramatically redistribution of intensity near the Bragg peaks. This redistribution is due primarily to long-range rotations of the Bragg planes caused by unpaired dislocations.

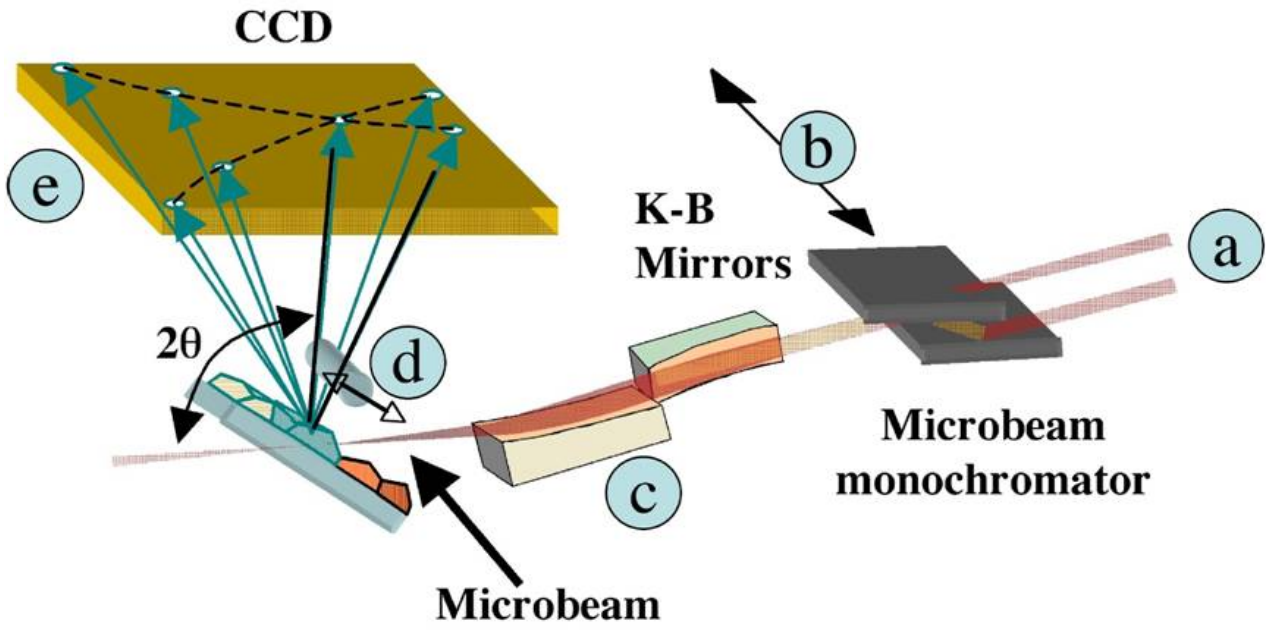

Fig. 4 Schematic of the 3D X-ray Crystal Microscope an instrument optimized for polychromatic microdiffraction experiments. The instrument includes (a)an ultra-brillant x-ray source; (b) a microbeam monochromator that can switch the beam from polychromatic to monochromatic radiation; (c) a nondispersive focusing Kirkpatrick-Baez mirror system; (d) a differential aperture for deconvolving the Laue patterns generated along the incident beam; and (e) an optimized x-ray sensitive area detector.

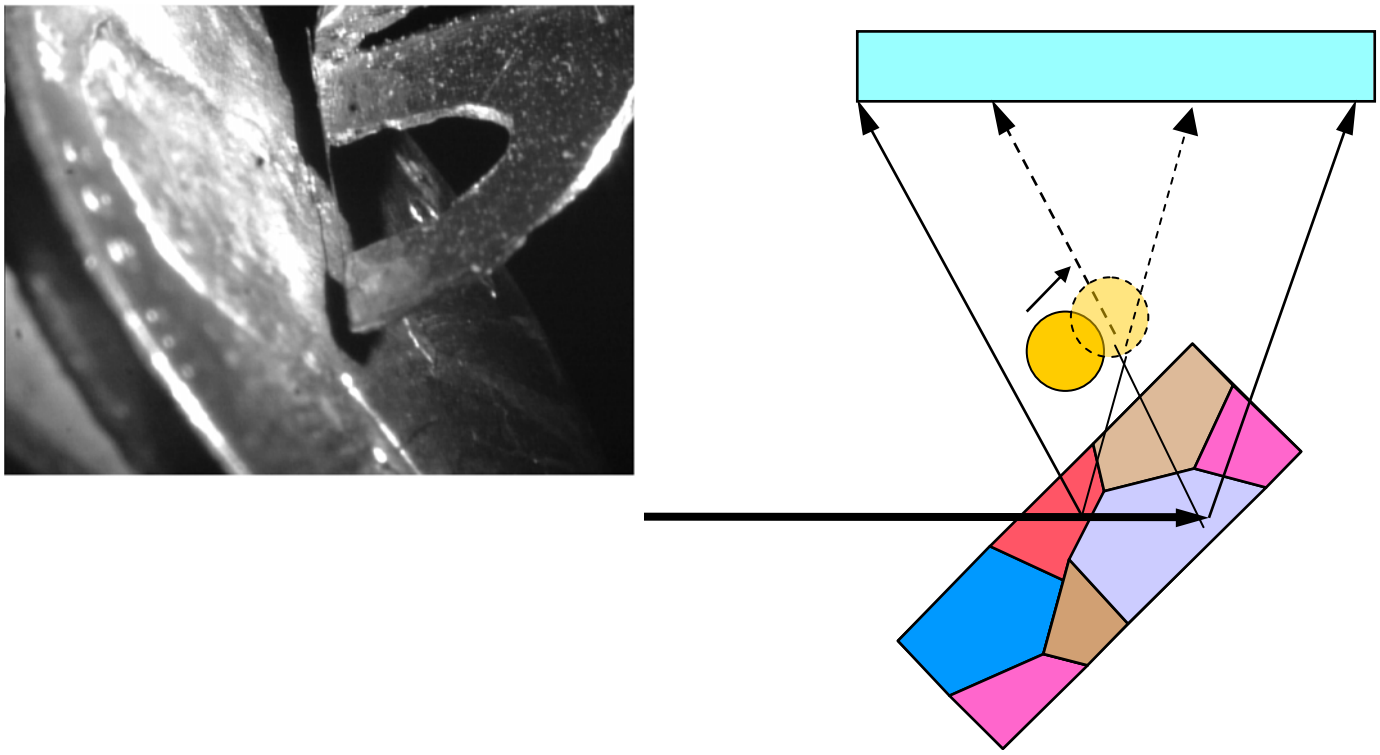

Fig. 5. Differential aperture. The intensity is monitored at each pixel as the wire is moved through the diffracted beam. The intensity origin for each pixel is determined by ray tracing back from the pixel position past the edge of the wire and onto the incident beam axis.

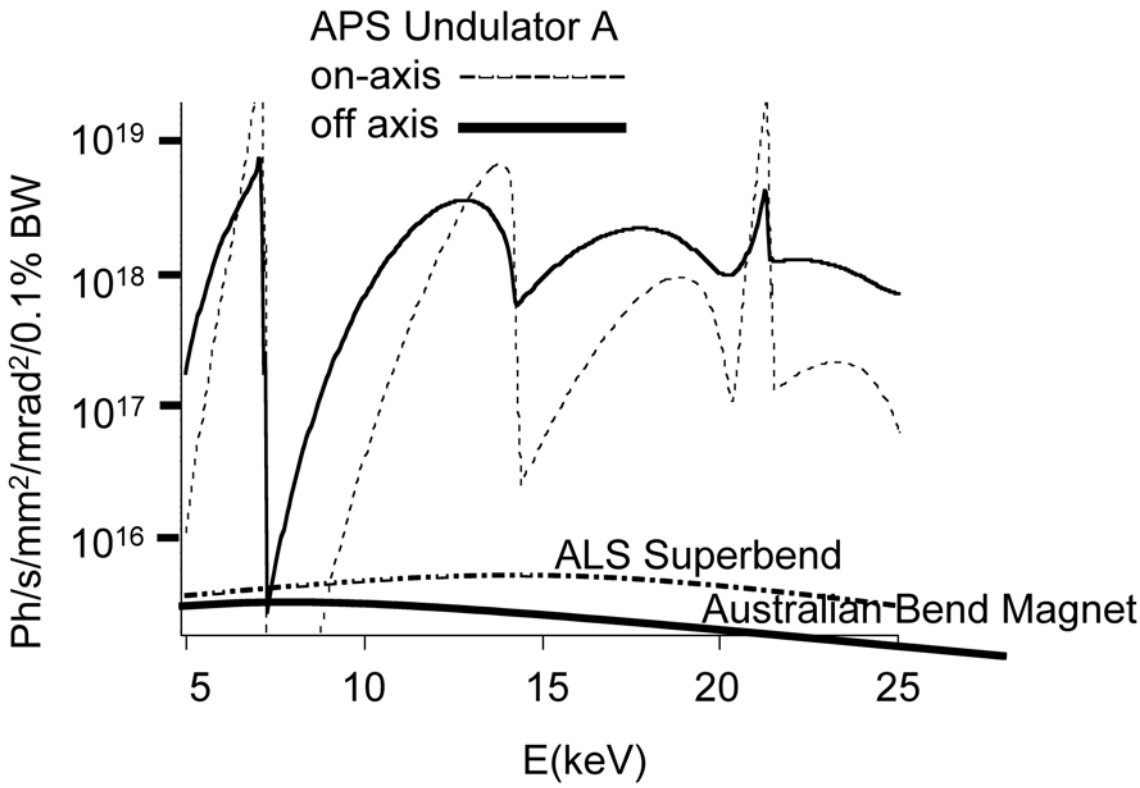

Fig. 6 Although a 3rd generation undulator source has about two orders of magnitude greater integrated brilliance than a bend magnet, the spectra has large fluctuations with wavelength that complicate polychromatic microdiffraction. Highest performance is achieved with an optimized undulator, but typically limitations in detector readout make bend magnet sources competitive for most experiments.

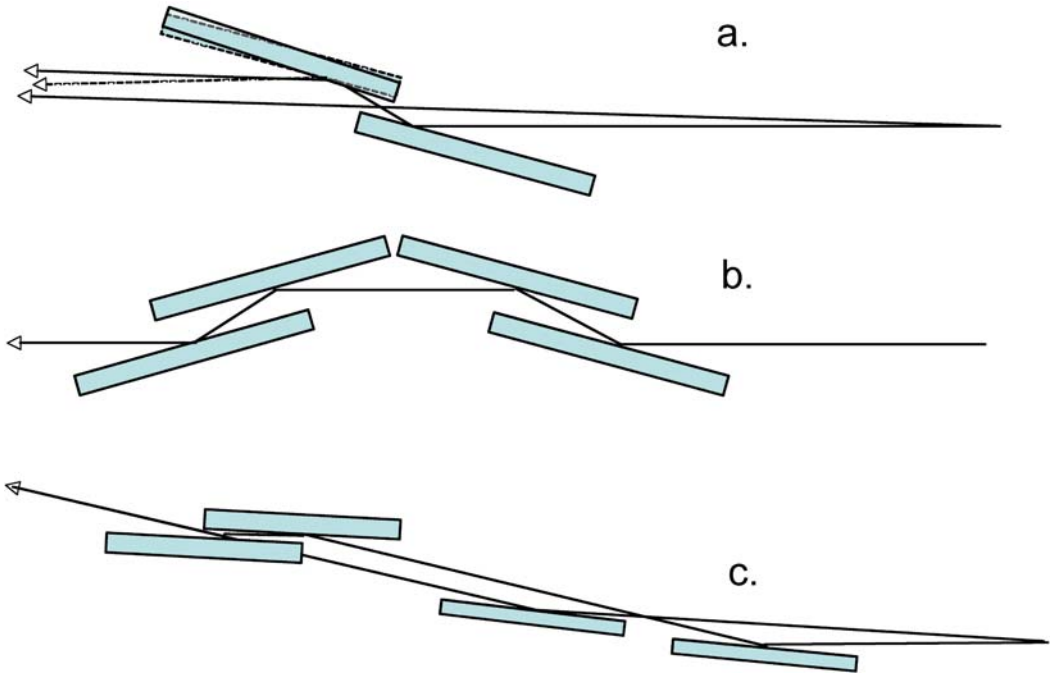

Fig. 7. a. Schematic of the microbeam monochromator on beamline 34-ID-E at the APS. The polychromatic beam is taken ~1 mm above the central beamline axis. This makes the polychromatic beam have a more uniform spectral intensity throughout the useful bandpass of the optics. B. The micromonochromator design on beamline 7 at the APS is a four crystal dispersive design that is intrinsically zero offset. C. The design for the VESPERS beamline at the Canadian light source uses mirrors and a small displacement monochromator to alternate between co-linear polychromatic or monochromatic beams.

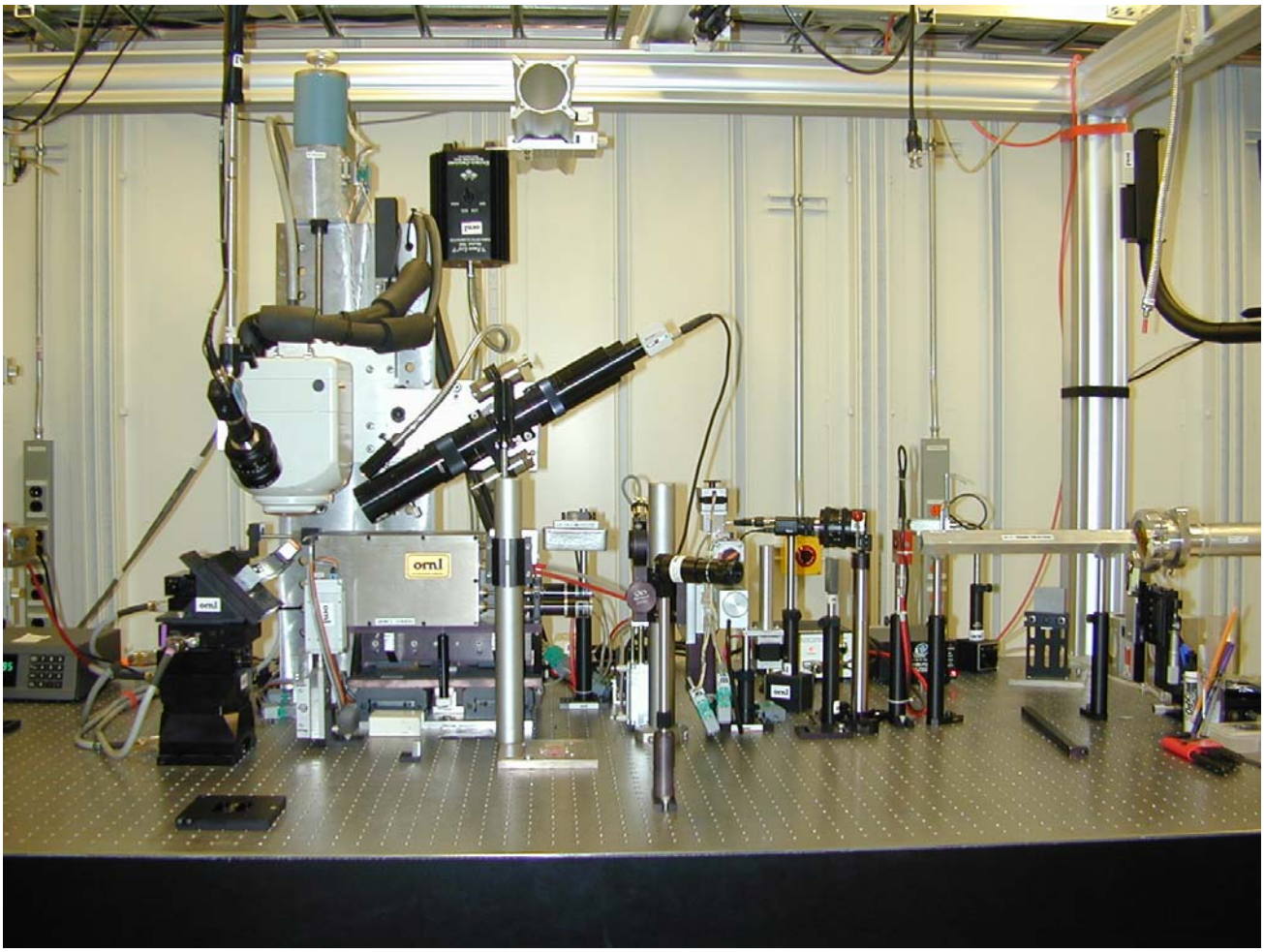

Fig. 8. The 3D X-ray crystal microscope on beamline 34-ID-E. The components are mounted on an optical table, which allows new optical approaches to be rapidly tested.

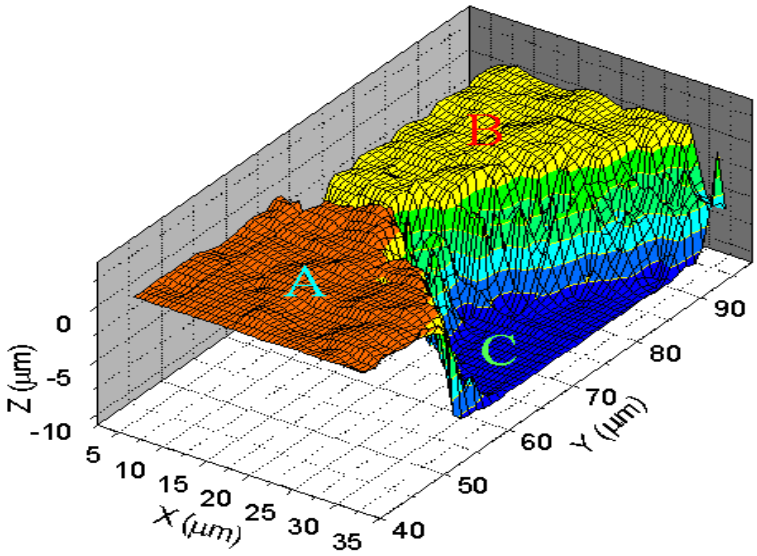

Fig. 9. The surface of a Ni triple grain junction color coded to show orientation of grains. The orientations were mapped by polychromatic microdiffraction and show grain boundary grooving, and a step in one of the grains surfaces. Internal grain boundary surfaces are also recovered with these measurements.

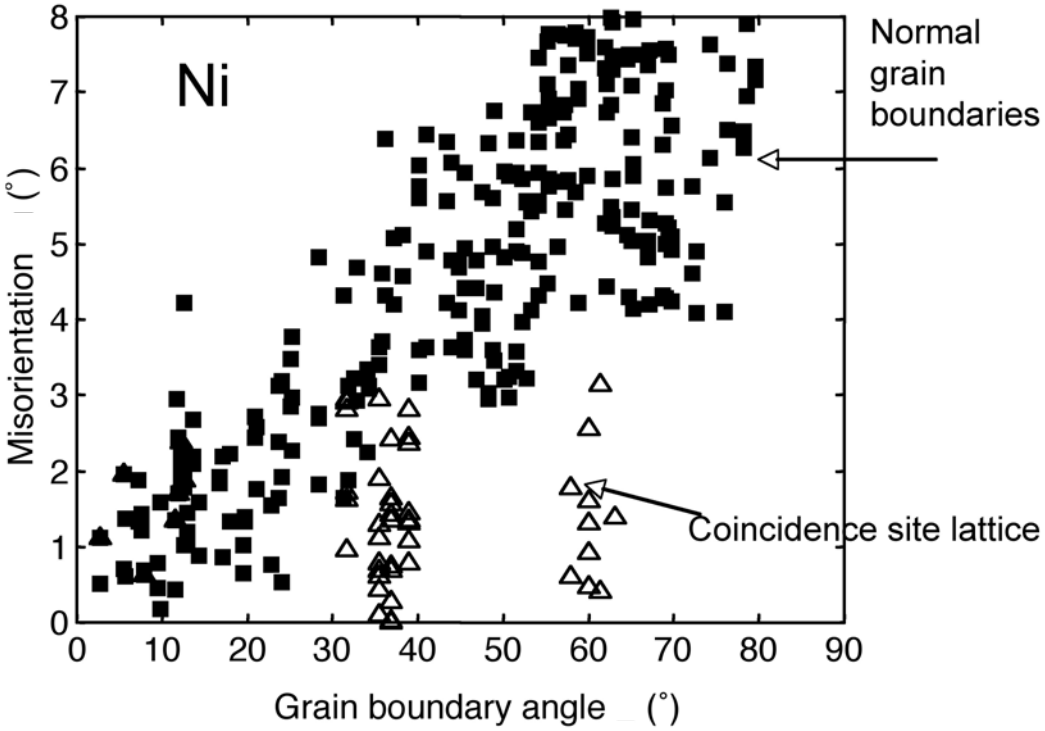

Fig. 10. Grain boundary angle before deformation (x-axis) compared to the change in misorientation across a grain boundary after deformation (y-axis). There is a positive correlation between grain boundary angle and misorientation during deformation. Grain boundary misorientations near coincidence site lattice boundaries however appear to have a distinctly different behavior from other boundaries.

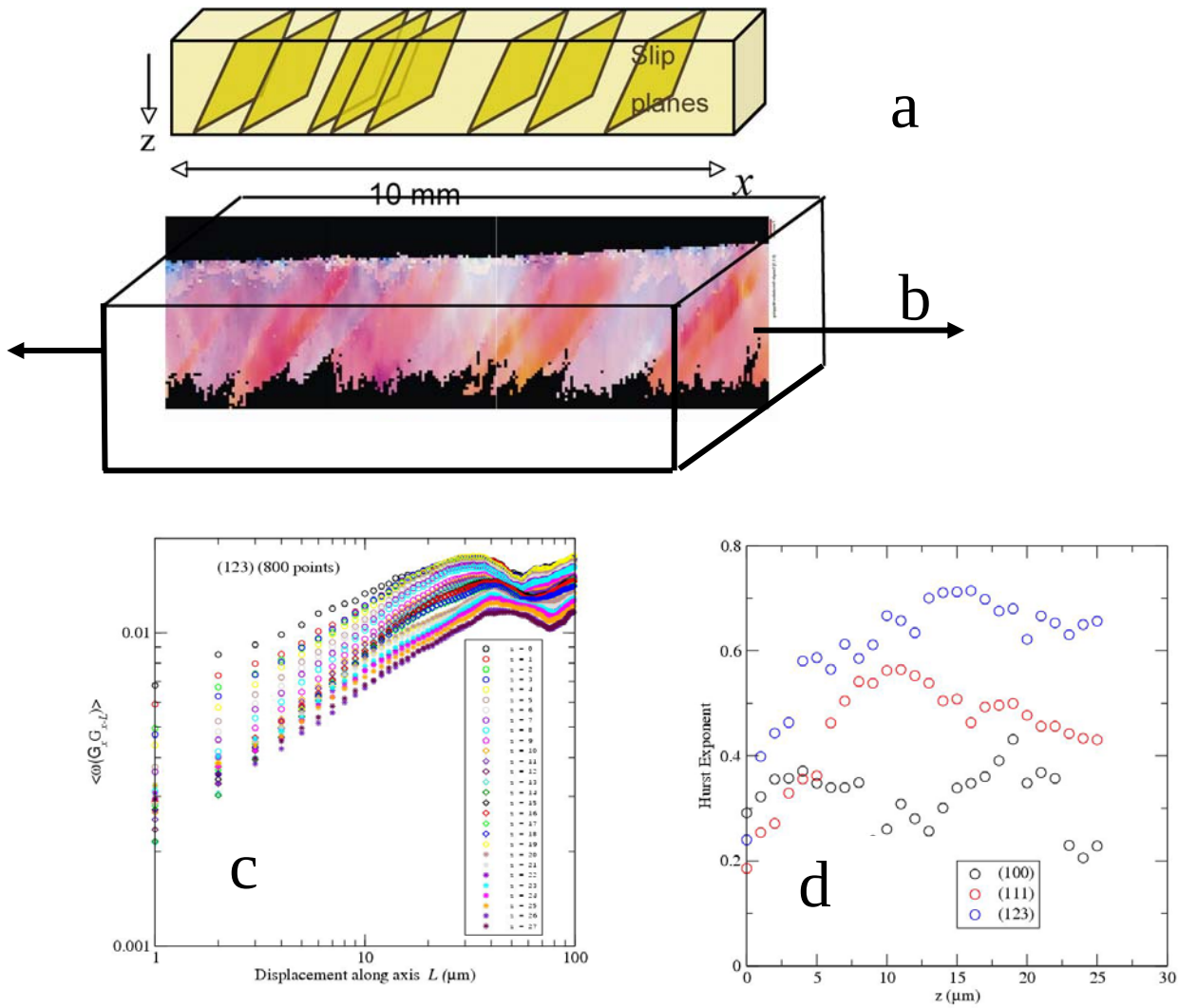

Fig. 11. a. Schematic of single crystal sample used to study deformation structure. Tensile specimens were pulled along various crystallographic orientations. Misorientations in points along the tensile specimen were studied as a function of depth and crystal orientation. A false color map (b) shows the orientation distribution in an interior surface of the sample. Hurst coefficient as a function of depth (c) and crystallographic orientation (d) indicate that both proximity to surface and crystal orientation effect the misorientation distribution of a deformed single crystal.

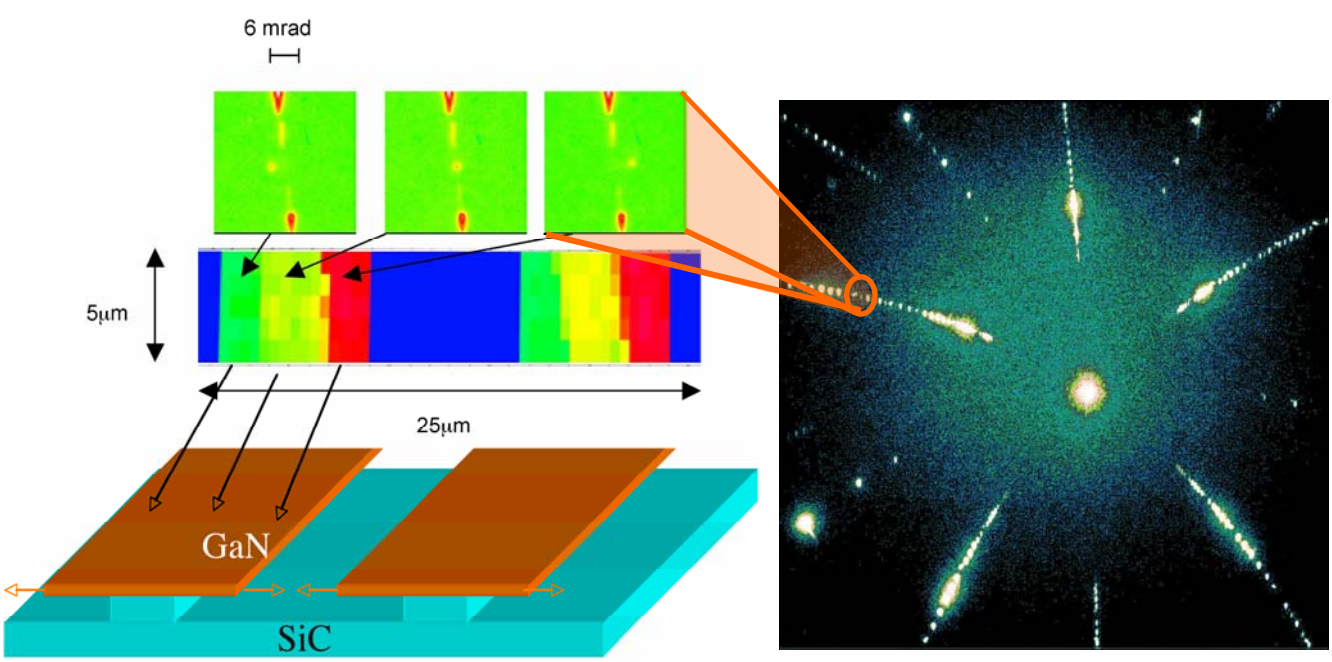

Fig. 12. The overall Laue image from this thin GaN film on SiC looks like a single crystal because the film is crystallographically aligned to the SiC substrate. A detailed look at individual reflections find that some are streaked (SiC) due to the finite penetration of the x-ray beam into the substrate. Other reflections change relative position depending on the location of the x-ray beam near pedestals etched into the substrate. These reflections are from the GaN film, which has wings tilted upward on each side of the pedestals.

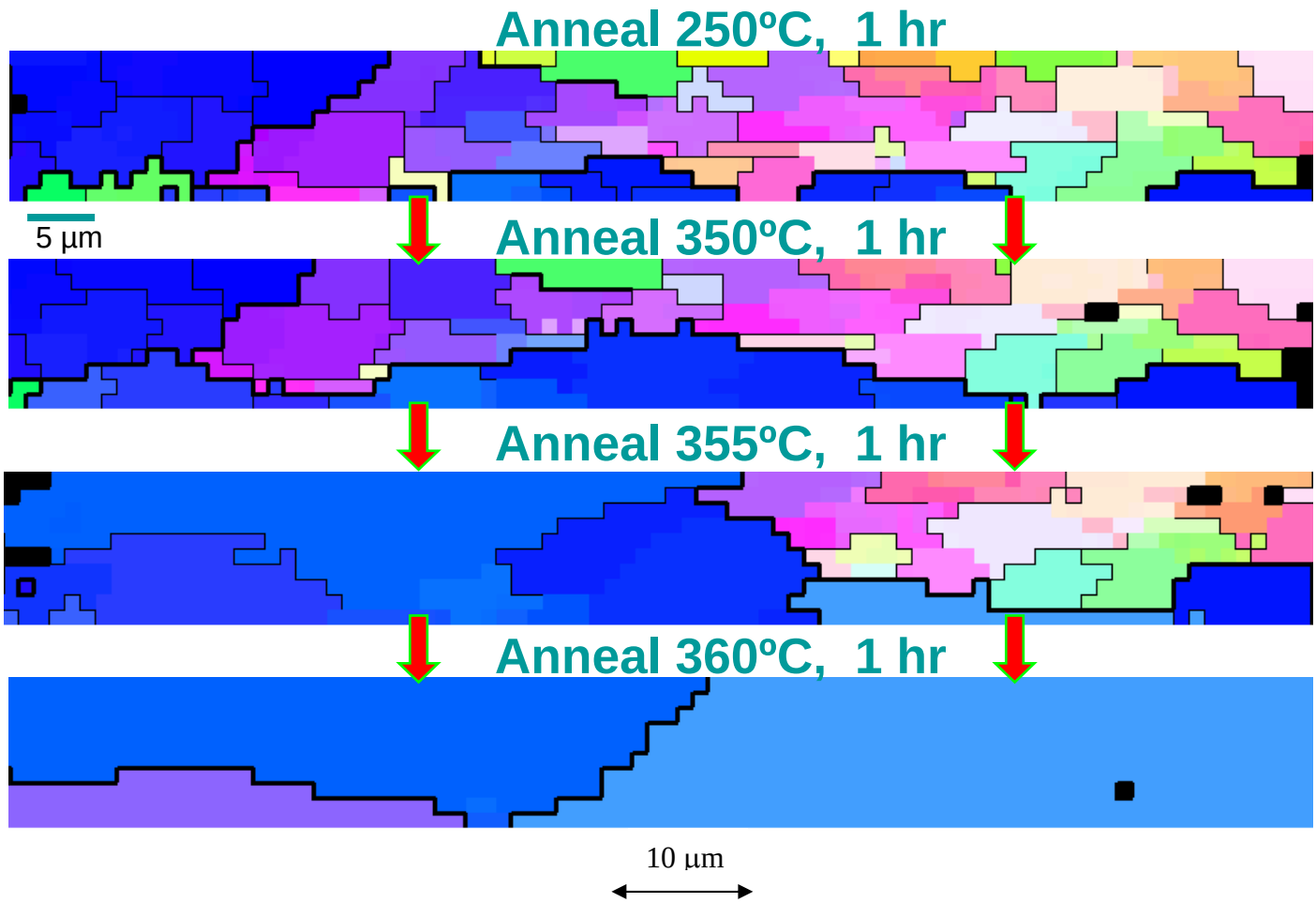

Fig. 13. Al grain structure at an interior sample surface before and after thermal annealing steps. The colors indicate crystal orientatin and the thickness of the lines indicates the misorientation across the grain boundary; the thicker the line the larger the misorientation.

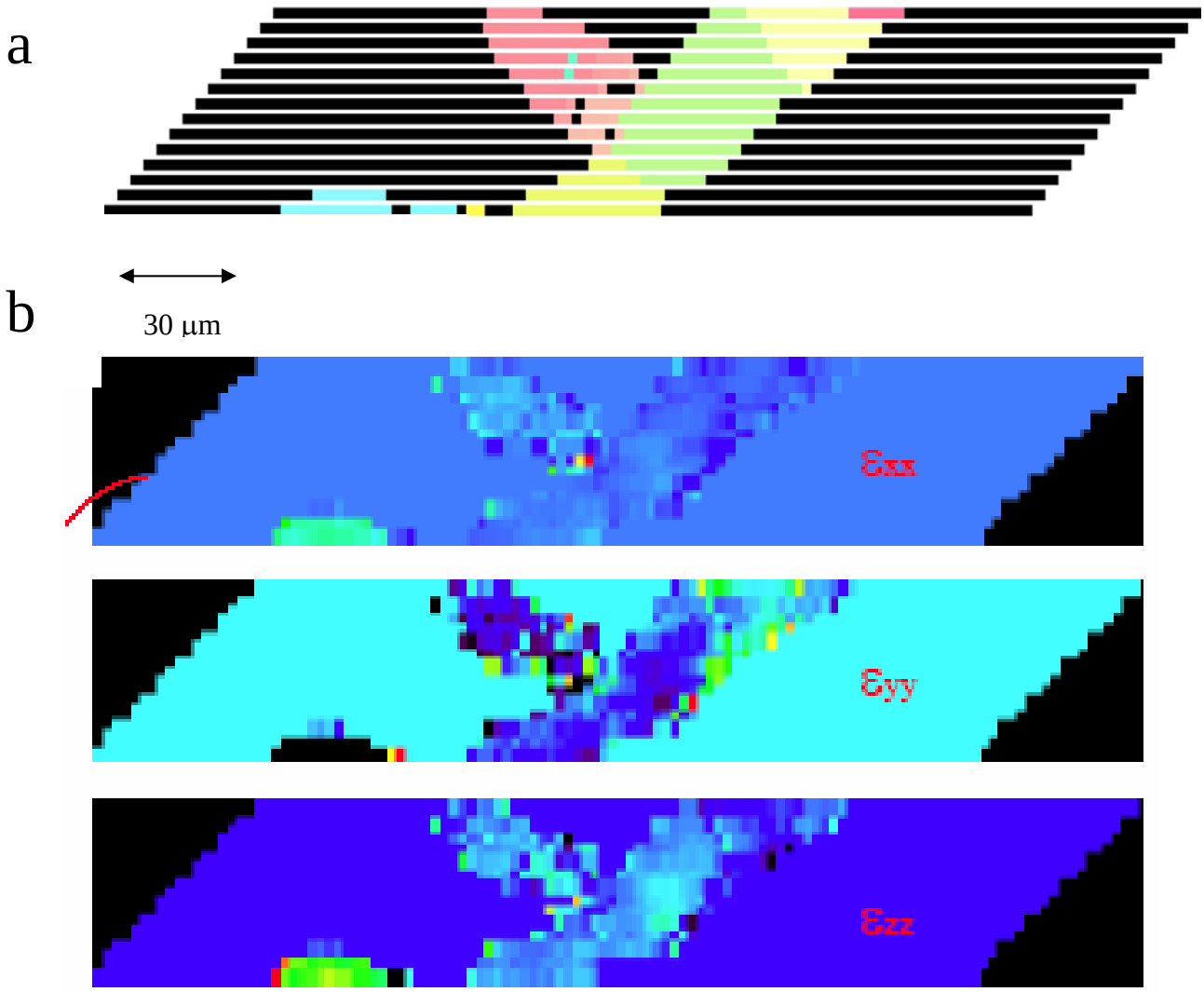

Fig. 14. (a) Cross section through a thin Sn film showing grain orientation and (b) grain elastic stress elements. Whiskers sticking out from the film are clearly visible near the lower left and center of the cross-sectional image.